Impacts of Projected Future Temperature Rise on the Hydrology of Neebing River, Ontario

by

Najiha Afnan

A thesis
submitted to the Faculty of Graduate Studies
in partial fulfillment of the requirements for the
Degree of Master of Science
in

Environmental Studies

Supervisor
Dr. Adam Cornwell
Associate Professor, Chair – Dept. of Geography & The Environment

Lakehead University
Thunder Bay, Ontario
April 2024

Abstract. The projected future temperature rise is likely to change the Neebing River's hydrology over the following decades. The changing hydrological patterns are expected to cause increased hydrological extremes in the City of Thunder Bay, Ontario. To safeguard this city from future climatic extremes, it is necessary to understand the Neebing River's hydrological response to anticipated future temperature rise and consider efficient prevention and long-term adaptation techniques. This study investigates the potential impacts of projected future temperature rise on the hydrology of the Neebing River Watershed and identifies potential mitigation and adaptation strategies. The Soil and Water Assessment Tool (SWAT) has been used to simulate the future streamflow for the period of 2041-2060 (near future), 2061-2080 (intermediate future), and 2081-2100 (distant future). The future air temperature and precipitation projections have been derived from three Global Climate Models (CanESM5, GFDL-ESM4, and INM-CM4-8) under medium (SSP2-4.5) and high (SSP5-8.5) emission scenarios. The SWAT model results reveal that compared to the baseline period of 2004-2023, the streamflow will increase significantly during the three future periods. There will be an increase in the winter, spring, and fall streamflow while a decrease in the summer streamflow. The results also suggest an increased intensity of future streamflow events. The findings of this study are expected to guide policy decisions intended to minimize damages from the unavoidable impacts of the projected future temperature rise. This study will also contribute to our understanding of the climate response of rivers in the Lake Superior basin and Northern Ontario in general.

Keywords: Future Temperature Rise, Hydrology, SWAT, Streamflow, Flooding Events.

1 Introduction

The Neebing River is located in the Thunder Bay District in Northwestern Ontario, Canada. This freshwater river runs through the City of Thunder Bay and the Municipality of Oliver Paipoonge. The river originates about 22 km northwest of Thunder Bay and flows in the southeast direction (Curi, 2018a). The thermal regime of this river falls into the coldwater category (average July temperature <17.5 °C) (Lakehead Region Conservation Authority, 2018; Jones and Schmidt, 2019). The Lakehead Region Conservation Authority (LRCA) is responsible for the management of the Neebing River Watershed (Lakehead Region Conservation Authority, 2018). The Neebing River contributes to the diverse geography of Thunder Bay. The river also offers several

recreational opportunities, including fishing, kayaking, wildlife watching, and walking trails along its banks.

The Neebing River has been periodically susceptible to flooding events which have caused significant damage to the City of Thunder Bay. A severe storm struck the region in 1941 which resulted in significant flooding along the river. The Neebing River also witnessed extensive storm-related flooding in 1968, 1971, and 1977. To mitigate flooding on the Neebing River, the Lakehead Region Conservation Authority (LRCA) built the Neebing-McIntyre Floodway in early 1983 (Rasid, 1988). After the construction of the floodway, the region experienced several major rainstorms in 1997, 2008, 2012, and 2016, but there was no riverine flooding. Nevertheless, the region experienced pluvial flooding during those years, which caused extensive damage (Curi, 2018b).

Canada has witnessed a significant rise in temperature over the past decades (Azarkhish et al., 2021). Greenhouse gas emissions are considered the main reason for the increasing temperature (Galata et al., 2021). Based on future projections, the temperature will continue to increase at a concerning pace over the 21st century (Marahatta et al., 2021). It is anticipated that this predicted rise in temperature will significantly impact river hydrology. Higher temperatures will lead to changes in precipitation patterns, and changes in the volume and intensity of precipitation will affect streamflow. A significant rise in temperature will change the timing and intensity of rainfall, which might result in more frequent and severe floods. Moreover, projected temperature rise might cause earlier and faster snowmelt that can alter the timing and magnitude of peak flows (Jiménez-Navarro et al., 2021).

In recent decades, there has been a remarkable increase in air temperature in the Neebing River basin. Future projections reveal that temperatures in the Neebing River basin will increase in the coming decades as well. Table 1 describes the annual average temperature projections of the Neebing River basin under high (SSP5-8.5) emission scenarios made available through ClimateData.ca (2024). Figure 1 illustrates the projected annual mean temperature of the Neebing River Basin for 2020-2100 under high (SSP5-8.5) and medium (SSP2-4.5) emission scenarios. The data presented in Table 1 and Figure 1 are the results of an ensemble of 24 distinct climate models. These values correspond to the ~10 km x 6 km grid cell where the Neebing River is situated. This is the resolution for downscaled data from all of the climate models.

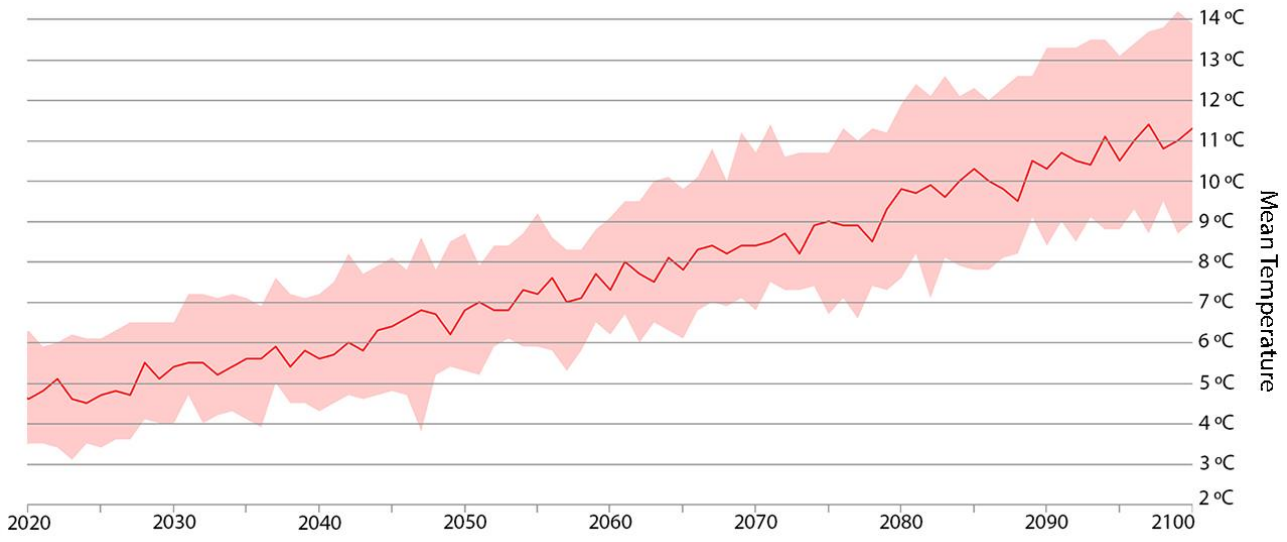

(a)

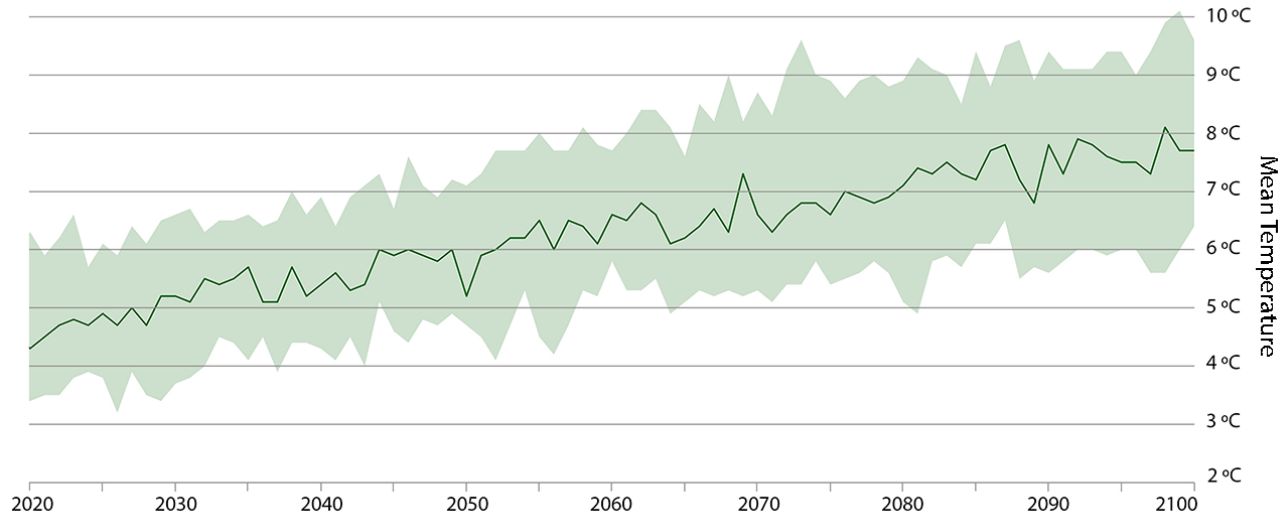

(b)

Fig. 1 Projected Annual Mean Temperature of Neebing River Basin for 2020-2100 under (a) high (SSP5-8.5) and (b) medium (SSP2-4.5) emission scenarios. The bold line indicates the median, while the shaded area depicts the range between the 10th and 90th percentiles of the ensemble (ClimateData.ca, 2024).

Table 1 Annual Average Temperature Projections of Neebing River basin, based on data from ClimateData.ca (2024).

Time Period	Annual Average Temperature
1971-2000	2.9 ºC
2021-2050	5.4 ºC
2051-2080	7.8 ºC
2071-2100	9.7 ºC

The Neebing River's hydrology could be vulnerable to the anticipated future temperature rise which might impact the whole drainage basin in an adverse way. Since the Neebing River flows into the urban area of Thunder Bay, urban life might be impacted as well. Therefore, it is important for the local authorities and decision-makers to analyze the future hydrologic changes under projected temperature rise and take necessary steps to minimize the damages from the unavoidable potential impacts.

2 Literature Review

2.1 Shared Socio-economic Pathways (SSPs)

The scenarios that illustrate the projections of socioeconomic changes around the world resulting from climate change throughout the year 2100 are known as the Shared Socioeconomic Pathways (SSPs) (Lee et al., 2021). The five Shared Socio-economic pathways are SSP1, SSP2, SSP3, SSP4, and SSP5. SSP1 refers to a tendency toward more sustainable behaviors, SSP2 indicates the continuation of past trends with few modifications, SSP3 and SSP4 represent more negative trends and limited human advancement, whereas SSP5 indicates fossil-based growth (Tehrani et al., 2022). The IPCC's Sixth Assessment Report focuses on five SSP-based scenarios (Lee et al., 2021). Table 2 describes these five scenarios. These scenarios illustrate a range of feasible greenhouse gas concentrations in the future and facilitate researchers and policymakers in exploring possible adaptation and mitigation against the potential impacts (Riahi et al., 2017).

Table 2 Five SSP-based scenarios that are focused on in the IPCC's Sixth Assessment Report (Lee et al., 2021).

Scenarios	SSP	Expected Radiative Forcing Level by 2100 ($W/m^{2)}$	GHG emissions	CO_2 emissions
SSP1-1.9	1	1.9	extremely low	will reach net zero by 2050
SSP1-2.6	1	2.6	low	will reach net zero by 2075
SSP2-4.5	2	4.5	medium	approximately as of right now through 2050 and will decline after 2050
SSP3-7.0	3	7.0	high	will have doubled around 2100
SSP5-8.5	5	8.5	very high	will have tripled around 2075

2.2 Global Climate Models (GCM)

The Global Climate Models (GCMs) are employed to simulate the global climate system and project future scenarios. GCMs are essential for evaluating the potential consequences of climate change worldwide. GCMs are capable of being run under different greenhouse gas (GHG) emission scenarios. Today, there are numerous GCMs, and GCM simulations have become an integral part of climate research worldwide (Provenzale, 2014).

2.3 Hydrological Modelling

Hydrological models are used to study the impacts of climate change on hydrology (Galata et al., 2021). Hydrological models not only assess the present scenarios but also the future scenarios that allow us to take appropriate measures (Pérez-Sánchez et al., 2020). The Soil and Water Assessment Tool (SWAT) is a hydrological model that is used globally for hydrological assessment (Daggupati et al., 2018). SWAT is capable of modeling large-scale watersheds (larger than 100 km^2) (Galata et al., 2021). SWAT model input data include DEM, land cover, soil, climate, and hydrological data (Daggupati et al., 2018). At first, the watershed is split up into several sub-watersheds by the SWAT model. Hydrologic Response Units (HRUs) are then created by subdivision of such sub-watersheds. Each HRU has distinct soil, slope, and land use features. SWAT uses the following water balance equation (Fatehifar et al., 2021).

$$SW_t = SW_0 + \sum_{i=1}^{t}(R_{day} - Q_{surf} + E_a - W_{seep} - Q_{gw})$$

SW_t- final soil water content (mm)

SW_0 - initial soil water content (mm)

t- time (days)

R_{day}- precipitation on day i (mm)

Q_{surf}- surface runoff on day i (mm)

E_a- evapotranspiration on day i (mm)

W_{seep}- percolation on day i (mm)

Q_{gw}- baseflow on day i (mm)

Over the last few decades, numerous studies have been conducted worldwide regarding the climate change impacts on hydrological processes. Table 3 summarizes the key findings of some of those studies.

Table 3 Selected articles on the impacts of climate change on hydrology using SWAT.

Authors	Watershed	Key Findings
Galata et al. (2021)	Hangar Watershed, Ethiopia	➢ Compared to the baseline period (1987–2017), in 2025-2055 the average annual runoff may increase by 24.5% under RCP 4.5 and 23.6% under RCP 8.5. ➢ In 2056-2086, the average annual runoff may increase by 23.6% and 73.2% under RCP 4.5 and 8.5, respectively.
Shrestha et al. (2018)	Songkhram River Basin, Thailand	➢ Compared to the baseline period (1990-2009), under RCP 4.5 scenario, the average streamflow is expected to decrease by 20%, 14.4%, and 24.1%, and under RCP 8.5, 22%, 18.7%, and 30.9% during the 2010–2039, 2040–2069, and 2070–2099 periods, respectively. ➢ Streamflow is expected to increase during winter and expected to decrease during the summer and rainy seasons.
Jiménez-Navarro et al. (2021)	Lake Erken Basin, Sweden	➢ Compared to the baseline period (1990–2014), in 2076-2100, the discharge will increase by around 18% in the SSP2-45 scenario, and 49% in the SSP5-85 scenario. ➢ In the SSP5-85 scenario, snow water equivalent (SWE) will be reduced by 38%-61% in 2026-2100, and 92% in 2076-2100.

		➢ Warmer temperatures in December, January, and February would lead to a decrease in snowfall and the accumulation of snow. Consequently, the SWE would be reduced by nearly 95% in the SSP5-85 scenario.
Marahatta et al. (2021)	Budhigandaki River Basin, Nepal	➢ Compared to the baseline period (1983–2012), the long-term average annual flows will increase between 21% and 25% in RCP 4.5 and 20% and 48% in RCP 8.5.
Saddique et al. (2019)	Jhelum River Basin, Pakistan	➢ Most of the GCMs suggested that compared to the baseline period (1976–2005), under RCP 4.5 and RCP 8.5, the annual streamflow would increase from 7.57% to 32.12% at the end of the 21st century.

2.4 Flood Disaster Management

Flooding is one of the most impactful natural disasters worldwide (Nordbeck et al., 2019). Floods lead to economic, social, and environmental losses. Strategic planning can mitigate flood damages before, during, and after a flood event. Flood disaster management tasks are undertaken by government entities, non-governmental organizations, and private agencies. Different stakeholders, including urban planners, civil engineers, environmentalists, architects, etc., should be involved in flood disaster management activities (Tingsanchali, 2012).

2.5 Structural, Non-structural, and Hybrid Strategies

Numerous structural, non-structural, and hybrid strategies have been adopted and implemented worldwide over the past decades to address flooding. Table 4 summarizes some of the flood control measures adopted and implemented by different cities around the world.

Table 4 Different flood control strategies adopted and implemented worldwide.

Authors	Flood Control Strategies
Rasid and Haider (2002) and McNeil, D. and Carson (2006)	➢ In Winnipeg, Manitoba, the Red River Floodway was built in 1968. The bypass channel, spanning 48 km, redirects floodwater from the City of Winnipeg. The floodway was expanded in 2005 to enhance flood protection.
Hamlin and Nielsen-Pincus (2021)	➢ Portland, Oregon constructed bioswales and big pipes for conveying flood water.
	➢ Eugene, Oregon constructed a concrete flood control channel spanning 2.8 km, and segments of the concrete channel had been turned into a a water-

	transporting vegetated channel to adopt a more environmentally sustainable solution.
	➢ Sherwood, Oregon safeguarded around 135 hectares of floodplains in a span of five years by restricting further developments.
	➢ Prineville, Oregon built a plant for processing wastewater mechanically.
Opperman et al. (2011)	➢ The Yolo Bypass, California is a classic example of floodplain reconnection. During flood events, additional flood-control infrastructure would have been needed in the absence of the Bypass.
Nordbeck et al. (2019)	➢ The Lower Austria government had created a surface runoff hazard map that offers detailed information about hazards. According to the building code, the living room floors should be elevated by a minimum of 30 cm above flood levels expected to occur once a century. Moreover, flammable liquids should be kept in a way that is resistant to flooding.
Godber (2006)	➢ In the Guragunbah urban floodplain, Australia, there are flood markers indicating the water levels recorded during past flood incidents in certain local government areas.
Poussin et al. (2012)	➢ In the Meuse river basin, Netherlands, an inundation model known as the Floodscanner model has been used to simulate future flood levels, and a damage model named the Damagescanner model has been used to evaluate future flood damage.
Minea et al. (2011)	➢ In the Bâsca River Catchment, Romania, the construction of a water reservoir and an underground system connected to it for accumulating water was started in 2007.
Tucci et al. (1999)	➢ To mitigate flooding in two cities of Brazil, several flood control strategies including, flood maps, real-time flood forecasting, and levees were proposed.

2.6 Risk Perception and Environmental Risk

The way people perceive environmental risk is influenced by their emotions. Different individuals perceive the same circumstances differently and, as a result, respond to them differently (Keller et al., 2012). Culture shapes how people perceive environmental risks and engage in pro-environmental actions (Zeng et al., 2020). People who have a greater understanding of environmental risks tend to engage in more pro-environmental actions (Fleury-Bahi, 2008). Individuals cannot accurately assess environmental risks without having adequate environmental

knowledge (Saari et al., 2021). Since the community often poorly understands the technical language of environmental risk (Godber, 2006), it is necessary to communicate those risks in the simplest, most easily understood terms.

2.7 Climate Change and Adaptation Planning

The world has witnessed a significant rise in temperature over the past few decades (Saddique et al., 2019). In various parts of the world, more frequent and severe floods have been documented due to climate change (Pérez-Sánchez et al., 2020). It is anticipated that future climate change will exceed historical levels, leading to more frequent storms and flooding (Kiedrzyńska et al., 2015). Therefore, developing strategies against future flooding is urgently required. For efficient adaptation planning, it is crucial to have adequate knowledge about anticipated climate changes (Füssel, 2007).

3 Methodology

3.1 Study Area

The area of the Neebing River watershed is 233.240 km^2 (Ontario Ministry of Natural Resources and Forestry, 2023). Most of the watershed is located in the City of Thunder Bay and the Municipality of Oliver Paipoonge. A small portion of the watershed is in the Township of Ware (Curi, 2018c). The Neebing River is 55.7 km in length (Lakehead Region Conservation Authority, 2018). It consists of two main branches: the western branch, which drains the western portion of the watershed, is about 20 km, and the northern branch, which drains the northern portion, is about 25 km. Pennock Creek is the largest tributary of the Neebing River. It drains the southern part of the watershed (Curi, 2018a). The mean and maximum elevation of the watershed is 285.8 m and 501.39 m, respectively. The annual mean temperature is 2.88 ºC, and the annual precipitation is 707 mm (Ontario Ministry of Natural Resources and Forestry, 2023). There are two gauging stations (02AB008 & 02AB024) along the Neebing River that provide flows and water level values (Fig. 2). On May 28, 2012, during an intense storm, the 02AB008 station recorded the highest flow in the Neebing River (Curi, 2018b).

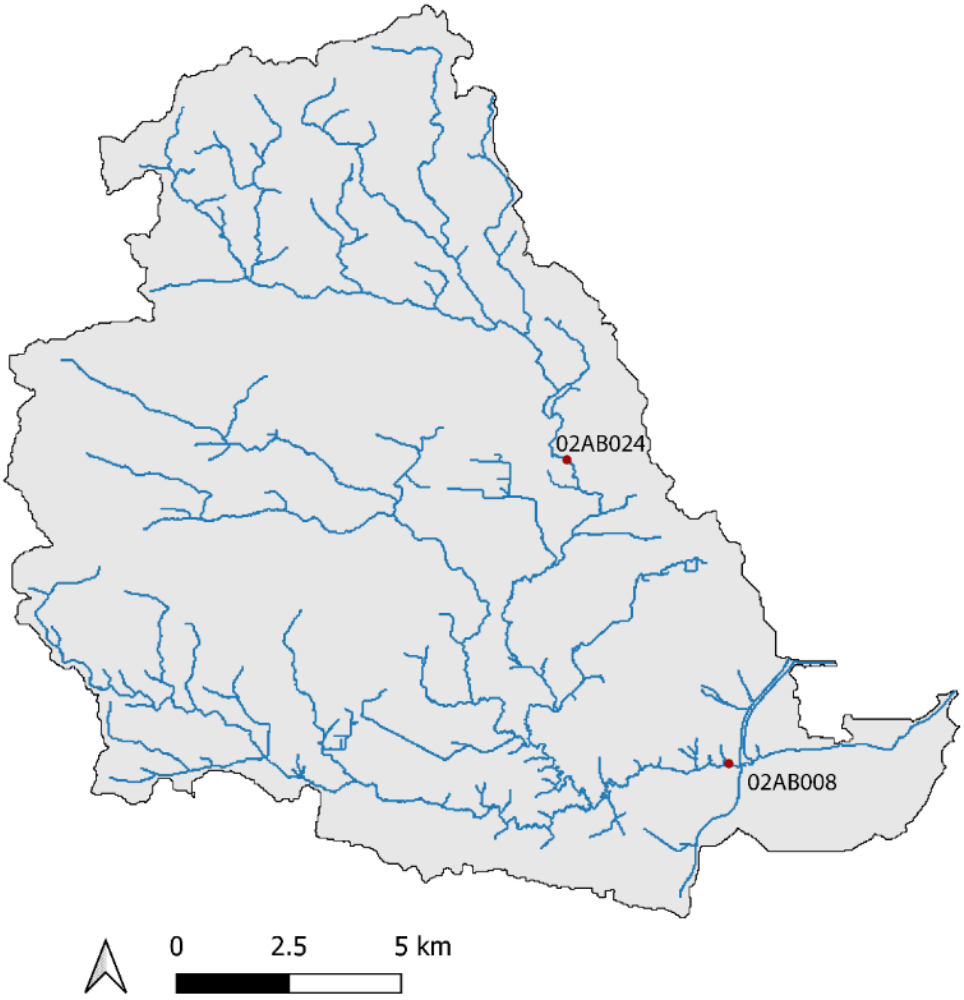

Fig. 2 Stream Network and Location of Two Gauging Stations (Ontario Ministry of Natural Resources and Forestry, 2023; Curi, 2018b).

3.2 SWAT Model Input Data

To simulate future hydrological scenarios, the SWAT model has been used in this study. The input data required for running the SWAT model include the digital elevation model (DEM), land cover, soil, climate, and hydrological data of the Neebing River watershed. Climate data include precipitation, maximum and minimum temperature, wind speed, relative humidity, and solar radiation. These input data have been derived from different international, domestic, and provincial databases.

3.2.1 DEM

The digital elevation model (DEM) of the Neebing River watershed has been derived from Ontario Ministry of Natural Resources and Forestry (2023). The DEM has a spatial resolution of 30 m. The DEM delineates the slopes and stream network of the watershed as well. The Neebing River watershed is generally a flat area with little slope variations (0%-21.41%). Figure 3(b) illustrates the slope variations of the study watershed.

3.2.2 Land Cover

Land cover data of the Neebing River watershed has also been extracted from Ontario Ministry of Natural Resources and Forestry (2023) at a spatial resolution of 30 m. The most dominant land cover of the study watershed is the treed area (77.251%), followed by the urban area (18.309%) and Agriculture & Rural Land Use (3.272%). Treed areas include sparse treed, deciduous treed, mixed treed, and coniferous treed. Other land cover includes clear open water and bog. The land cover data has been transformed in accordance with the SWAT code. Table 5 describes all the land cover types of the Neebing River watershed and their transformation to SWAT code.

Table 5 Land Cover Type Percentages and transformation to SWAT code.

Land Cover Type	SWAT Description	SWAT Code	% to Total
Sparse Treed	Savanna	SAVA	36.706
Deciduous Treed	Forest- Deciduous	FRSD	19.805
Mixed Treed	Forest-Mixed	FRST	17.196
Coniferous Treed	Forest-Evergreen	FRSE	3.544
Community/ Infrastructure	Residential, medium density	URMD	18.309
Agriculture & Undifferentiated Rural Land Use	Agricultural Land-Generic	AGRL	3.272
Bog	Wetlands-Mixed	WETL	0.642
Clear Open Water	Water	WATR	0.518

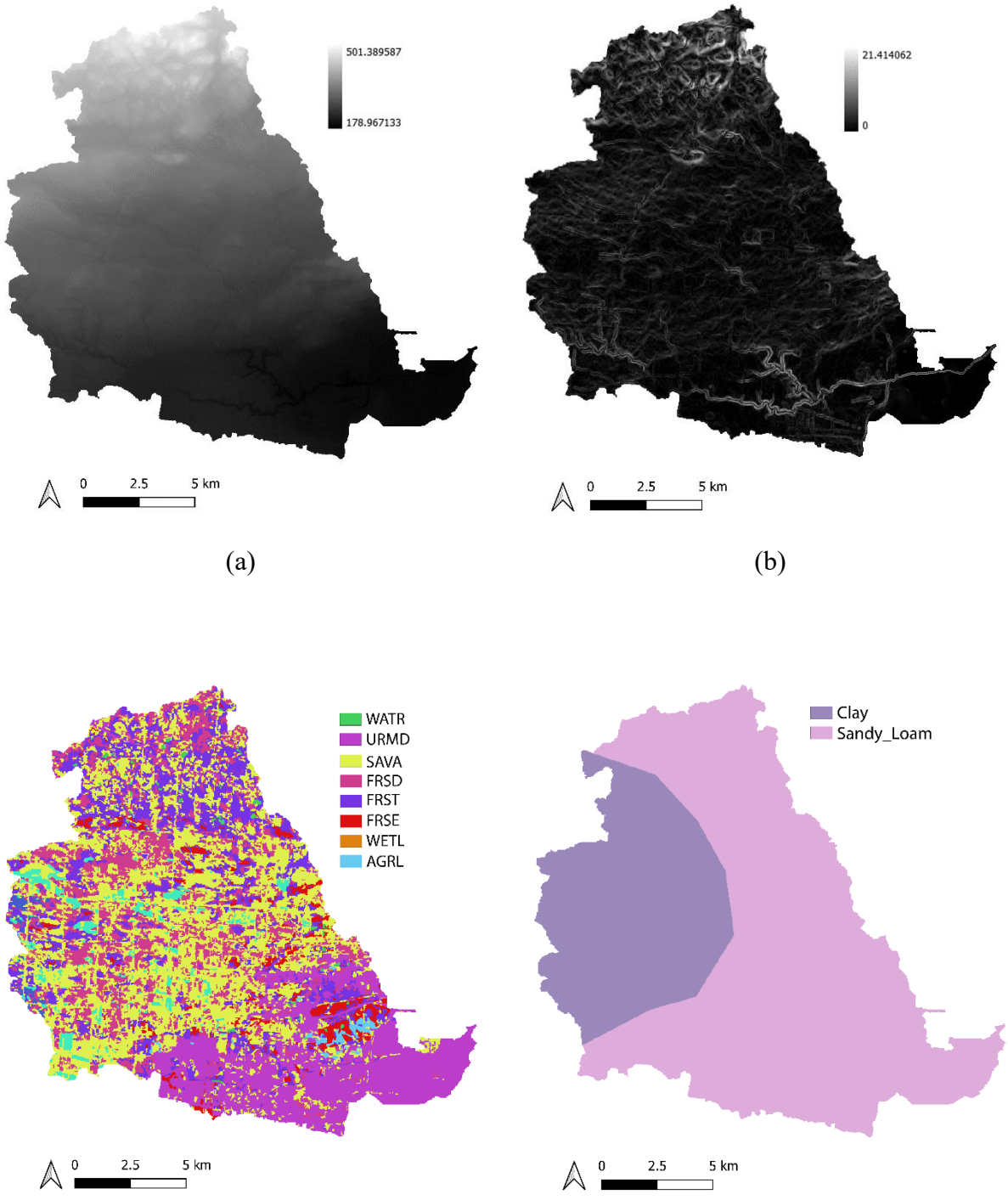

Fig. 3 (a) DEM, (b) Slope Variations, (c) Land Cover Map, and (d) Soil Map of the Neebing River Watershed (Ontario Ministry of Natural Resources and Forestry, 2023; Food and Agriculture Organization of the United Nations, 2023)

3.2.3 Soil

Soil data of the Neebing River watershed has been obtained from Food and Agriculture Organization of the United Nations (2023). The spatial resolution of the soil map is ~5 km. There are mainly two types of soil in the Neebing River watershed. The most dominant soil type is Sandy Loam (67.34%), and the other soil type present is Clay (32.66%). Figure 3(d) illustrates the soil map of the Neebing River watershed.

3.2.4 Climate Data

3.2.4.1 Historical Climate Data

Historical climate data for the period of 2004-2023 have been extracted from Environment and Climate Change Canada (2024a). Daily precipitation, maximum temperature, and minimum temperature data have been acquired from the "Thunder Bay CS" weather station (Latitude: 48°22'10.000" N, Longitude: 89°19'38.000" W, Climate ID: 6048268). This station provides a longer period of data and more recent data (2003-2024) than the other weather stations. The station provides hourly, daily, and monthly data.

3.2.4.2 Future Climate Data

Future climate data for the period of 2041-2060 (near future), 2061-2080 (intermediate future), and 2081-2100 (distant future) have been obtained from ClimateData.ca (2024). This website provides downscaled and bias-adjusted data collected from CMIP6 using the BCCAQv2 method (Gaspard et al., 2023). The forecasting period commenced in 2041 based on the relevant literature (Li et al., 2023; Zhang et al., 2023). The future air temperature and precipitation data have been acquired from three GCMs (CanESM5, GFDL-ESM4, and INM-CM4-8) under medium (SSP2-4.5) and high (SSP5-8.5) emission scenarios. In SSP2-4.5, future climate change challenges are lesser, whereas in SSP5-8.5, future climate change impacts are greater (Jiménez-Navarro et al., 2021). CanESM5 was chosen because it is a Canadian model, and the study site is in Canada. GFDL-ESM4 was chosen because it is a North American model (United States), and the study site is in North America. INM-CM4-8 was chosen because it is a Russian model, and the climatic conditions are similar in Russia and Canada. Besides, CanESM5, GFDL-ESM4, and INM-CM4-

8 are representative of the high, middle, and low climate sensitivities, respectively, among CMIP6 models (Zelinka et al., 2020). Table 6 describes the three GCMs used in this study.

Table 6 Three GCMs used in this study

CanESM5	Canadian Earth System Model 5	Canadian Centre for Climate Modelling and Analysis (CCCma), Canada
GFDL-ESM4	Geophysical Fluid Dynamics Laboratory Earth System Model 4)	National Oceanic and Atmospheric Administration (NOAA), United States
INM-CM4-8	Institute of Numerical Mathematics Coupled Model version 4.8	Institute for Numerical Mathematics, Russian Academy of Science, Moscow, Russia

3.2.5 Hydrological Data

Hydrological data have been derived from Environment and Climate Change Canada (2024b). The streamflow data for the period of 1953-2022 have been obtained from the "Neebing River Near Thunder Bay" station (Latitude: 48°23'00" N, Longitude: 89°18'23" W, Station Number: 02AB008, Gross Drainage Area: 187 km^2). This station provides daily, monthly, and annual data.

3.3 SWAT Model Setup

QSWAT, which is a QGIS interface for SWAT, has been employed in this research. At first, the stream network of the Neebing River basin was delineated by using a threshold area of 1.5 km^2. 89 sub-basins were created based on the stream network. In the next step, the Hydrologic Response Units (HRUs) were created by using land cover data, soil data, and slope classes. Slopes of the Neebing River basin were divided into five classes (0%–5%, 5%–10%, 10%–15%, 15%–20%, and >20%). 10% landuse, 10% soil, and 10% slope thresholds were used. Then, those 89 sub-basins were sub-divided into 492 Hydrologic Response Units (HRUs). The simulation of the model was conducted on a daily, monthly, and yearly basis, starting from 2004 to 2023.

3.3.1 Calibration & Validation of SWAT Model

The SWAT model output was calibrated and validated using the SWAT Calibration and Uncertainty Programs (SWAT-CUP) under the Sequential Uncertainty Fitting-2 (SUFI-2) method. Calibration and validation were conducted using the daily observed streamflow data at the "Neebing River Near Thunder Bay" station. The data were split into three periods: calibration (2011–2015), validation (2016–2020), and warm-up (2006–2010). The warm-up phase was included to enhance the efficiency of the model.

4 Results and Discussion

4.1 Sensitivity Analysis

Global Sensitivity Analysis has been conducted to determine the most sensitive SWAT parameters in this study. Sixteen parameters for streamflow were selected based on the relevant literature on sensitivity analysis (Asadzadeh et al., 2015; da Silva et al., 2015; Galata et al., 2021; Liu et al., 2016; Pérez-Sánchez et al., 2020; Rahman et al., 2012; Saddique et al., 2019; Shrestha et al., 2018). A preliminary simulation was conducted in SWAT-CUP to identify which parameters were the most sensitive in simulating the streamflow of the Neebing River Watershed. Thirteen parameters were found to which the model was most sensitive. Table 7 describes the results of the sensitivity analysis. The parameters with the lowest *p*-value and the highest t-stat value are the most sensitive (Pérez-Sánchez et al., 2020). Adjustments were made to these parameters at the conclusion of every iteration during the calibration process. Subsequently, the calibrated parameters were applied during the validation process.

Table 7 Sensitivity Analysis of SWAT Model Parameters.

SWAT Parameter	t-Stat	*p*-value	Sensitivity	Rank
v_CH_K2.rte	28.993235478	0.000000000	High	1
v_CH_N2.rte	27.016779375	0.000000000	High	2
r_CN2.mgt	-22.206167473	0.000000000	High	3
v_ESCO.hru	-8.919992125	0.000000000	High	4

v_SMFMX.bsn	-7.544348784	0.000000000	High	5
v_ALPHA_BF.gw	-6.281995212	0.000000000	High	6
v_SMTMP.bsn	4.500119682	0.000007185	High	7
v_SFTMP.bsn	-4.319335451	0.000016423	High	8
r_SOL_AWC.sol	3.900376387	0.000099243	High	9
v_SURLAG.bsn	-1.990125303	0.046714234	High	10
v_GWQMN.gw	-1.832325758	0.067052790	High	11
v_TIMP.bsn	-1.790946616	0.073454331	High	12
v_SMFMN.bsn	-1.436486485	0.151021700	High	13
v_GW_DELAY.gw	0.827518071	0.408043055	Low	14
v_EPCO.hru	-0.722346381	0.470166718	Low	15
r_SOL_K.sol	-0.219225247	0.826497151	Low	16

4.2 Performance of SWAT Model

The efficiency of the SWAT model has been estimated using three model performance statistics: coefficient of determination (R^2), Nash–Sutcliffe coefficient (NSE), and percent bias (PBIAS). During calibration (2011-2015), the obtained values are $R^2 = 0.62$, NSE =0.61, PBIAS = -5.8, and during validation (2016-2020), the obtained values are $R^2 = 0.61$, NSE = 0.60, PBIAS = 0.2. Table 8 describes the performance rating of R^2, NSE, and PBIAS during calibration and validation of the SWAT model.

Table 8 Performance Rating of R^2, NSE, and PBIAS (Carlos Mendoza et al., 2021).

R^2	**NSE**	**PBIAS**	**Rating**
$0.75< R^2 \leq 1.00$	$0.75< R^2 \leq 1.00$	PBIAS $\leq \pm 10$	Very good
$0.60< R^2 \leq 0.75$	$0.60< R^2 \leq 0.75$	$\pm 10 <$ PBIAS $\leq \pm 15$	Good
$0.50< R^2 \leq 0.60$	$0.36< R^2 \leq 0.60$	$\pm 15 <$ PBIAS $\leq \pm 25$	Satisfactory

The results demonstrate a good efficiency of the SWAT model in daily streamflow simulation of the Neebing River watershed, and it can be employed to simulate future streamflow with confidence.

The observed daily streamflow data have been compared with the simulated data. During both the calibration and validation periods, the observed and simulated daily streamflow shows a strong correlation. Figure 4 illustrates the observed and simulated daily streamflow during the calibration and validation periods.

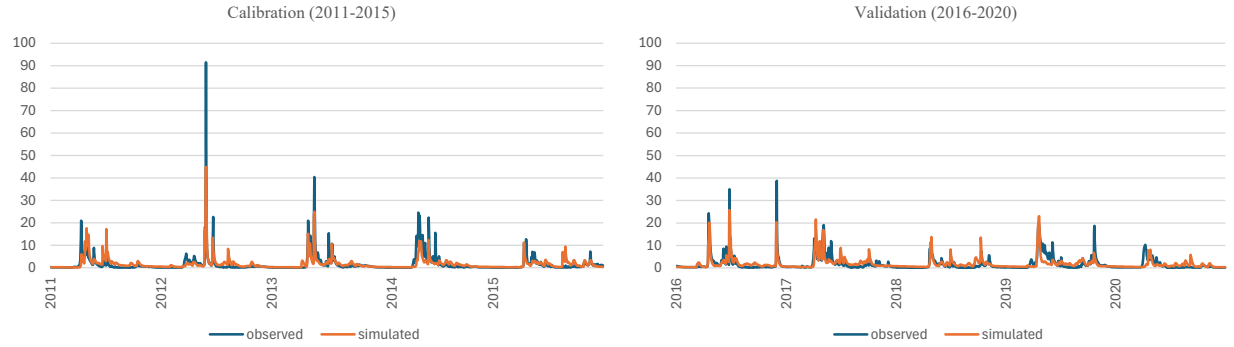

(a) (b)

Fig. 4 Comparison between observed and simulated daily streamflow during (a) calibration and (b) validation periods.

4.3 Changes in Future Climate

The future changes in maximum and minimum temperatures and precipitation have been estimated by comparing the climatic data of the near, intermediate, and distant future periods with the climatic data of the baseline period. The bias-corrected data from three GCMs (CanESM5, GFDL-ESM4, and INM-CM4-8) for the period of 2041-2060, 2061-2080, and 2081-2100 under two emission scenarios (SSP2-4.5 and SSP5-8.5) have been compared with the climatic data of the observed baseline period (2004-2023). Table 9 describes the average annual maximum and minimum temperatures and precipitation of three GCMs during the near, intermediate, and distant future periods under both emission scenarios.

According to all three GCMs, the average annual maximum and minimum temperatures will increase during the near, intermediate, and distant future periods under both emission scenarios compared to the observed baseline period. The average annual precipitation is also projected to increase during the future periods under both emission scenarios. As anticipated, the SSP5-8.5 projections for maximum and minimum temperatures and precipitation are greater than the SSP2-4.5 projections. The highest increase in maximum temperature is 8.59 ºC, which is projected by

CanESM5 during the 2081-2100 period under SSP5-8.5. The highest increase in minimum temperature is 10.98 ºC, which is projected by CanESM5 during the 2081-2100 period under SSP5-8.5. The highest increase in precipitation is 33.88%, which is projected by CanESM5 during the 2081-2100 period under SSP5-8.5.

Table 9 The average annual maximum and minimum temperatures and precipitation during 2041-2060, 2061-2080, and 2081-2100 under SSP2-4.5 and SSP5-8.5.

GCM	SSP	Period	Maximum Temperature (ºC)	Minimum Temperature (ºC)	Precipitation (mm/d)
Baseline (2004-2023)			9.47	-2.83	1.74
CanESM5	2-4.5	2041-2060	12.34	1.83	2.20
		2061-2080	13.57	3.27	2.16
		2081-2100	13.75	3.45	2.16
	5-8.5	2041-2060	13.31	3.01	2.15
		2061-2080	15.90	5.89	2.21
		2081-2100	18.06	8.15	2.33
GFDL-ESM4	2-4.5	2041-2060	10.70	-0.16	2.09
		2061-2080	11.30	0.33	2.06
		2081-2100	11.89	1.18	2.29
	5-8.5	2041-2060	11.23	0.45	2.10
		2061-2080	12.58	1.96	2.27
		2081-2100	14.32	3.70	2.22
INM-CM4-8	2-4.5	2041-2060	10.09	-0.59	2.02
		2061-2080	10.97	0.28	2.13
		2081-2100	10.94	0.35	1.95
	5-8.5	2041-2060	10.91	0.57	2.12
		2061-2080	12.59	2.32	2.11
		2081-2100	13.06	3.03	2.11

The absolute changes in maximum and minimum temperatures and relative change in precipitation during the future periods under both emission scenarios compared to the observed baseline period are illustrated in Figure 5.

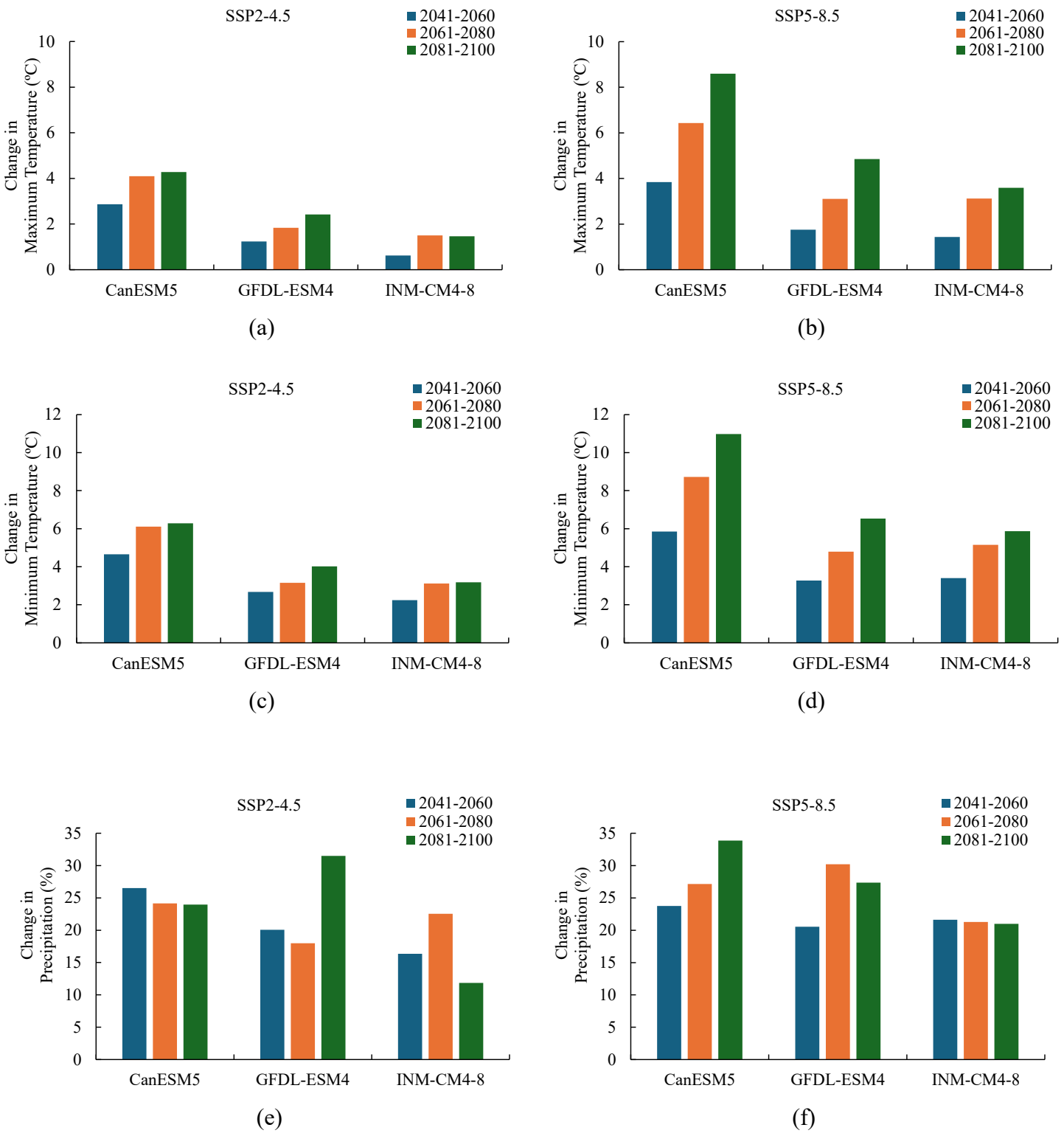

Fig. 5 The absolute changes in (a,b) maximum temperature, (c,d) minimum temperature, and relative change in (e,f) precipitation during 2041-2060, 2061-2080, and 2081-2100 under SSP2-4.5 and SSP5-8.5 in comparison to the observed baseline period (2004-2023).

4.4 Changes in Annual Streamflow

The future changes in annual streamflow have been estimated by comparing the simulated streamflow of the near, intermediate, and distant future periods under both emission scenarios with the simulated streamflow of the baseline period. The simulated average annual streamflow data from three GCMs (CanESM5, GFDL-ESM4, and INM-CM4-8) for the period of 2041-2060, 2061-2080, and 2081-2100 under SSP2-4.5 and SSP5-8.5 have been compared with the simulated average annual streamflow data of the baseline period of 2004-2023. Table 10 describes the simulated average annual streamflow and relative changes in the simulated average annual streamflow of three GCMs during the future periods under both emission scenarios compared to the simulated baseline period of 2004-2023.

Table 10 The average annual streamflow and relative change in average annual streamflow during 2041-2060, 2061-2080, and 2081-2100 under SSP2-4.5 and SSP5-8.5 compared to the simulated baseline period (2004-2023).

GCM	SSP	Period	Annual Streamflow (m^3/s)	% Change
Baseline (2004-2023)			2.15	
CanESM5	2-4.5	2041-2060	2.85	32.26
		2061-2080	2.94	36.59
		2081-2100	2.75	27.66
	5-8.5	2041-2060	2.91	34.91
		2061-2080	2.75	27.57
		2081-2100	3.23	49.76
GFDL-ESM4	2-4.5	2041-2060	2.76	28.13
		2061-2080	2.61	20.94
		2081-2100	2.59	20.17
	5-8.5	2041-2060	3.23	49.79
		2061-2080	3.19	48.20
		2081-2100	2.81	30.26
INM-CM4-8	2-4.5	2041-2060	2.70	25.13
		2061-2080	2.85	32.37
		2081-2100	2.86	32.75
	5-8.5	2041-2060	2.65	22.79
		2061-2080	2.49	15.46
		2081-2100	2.63	22.21

According to all three GCMs, the average annual streamflow is projected to increase during the near, intermediate, and distant future periods under both emission scenarios in comparison to the simulated baseline period. The highest increase in streamflow is 49.79%, which is projected by GFDL-ESM4 during the 2041-2060 period under SSP5-8.5, while the lowest increase is 15.46%, which is projected by INM-CM4-8 during the 2061-2080 period under SSP5-8.5. Figure 6 illustrates the absolute changes in the simulated average annual streamflow of three GCMs during the future periods under both emission scenarios compared to the simulated baseline period.

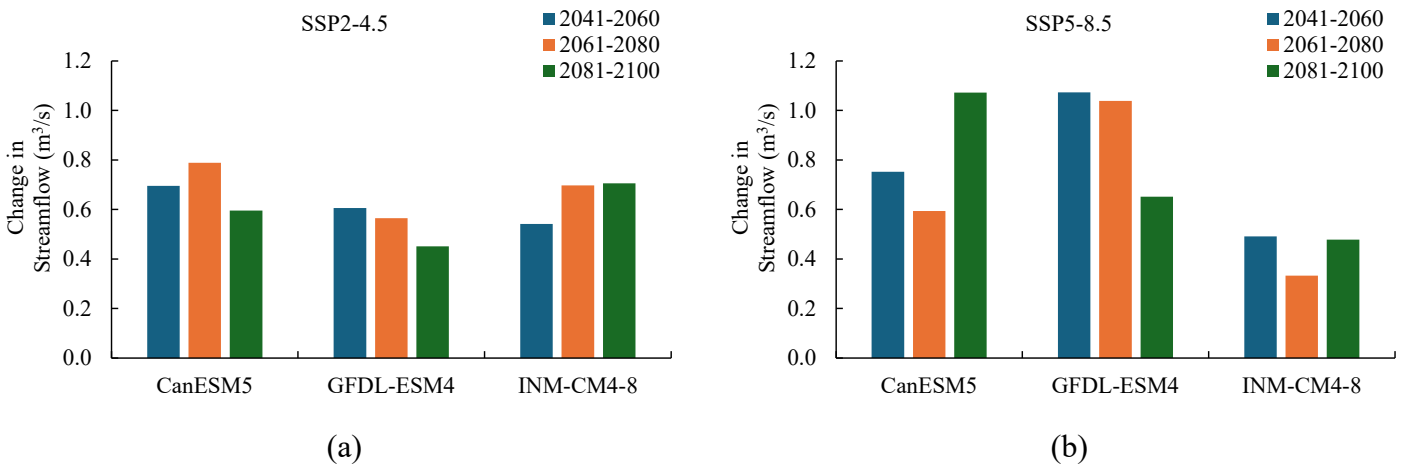

Fig. 6 The absolute changes in simulated average annual streamflow during 2041-2060, 2061-2080, and 2081-2100 under (a) SSP2-4.5 and (b) SSP5-8.5 compared to the simulated baseline period (2004-2023).

4.5 Changes in Seasonal Streamflow

The future changes in seasonal streamflow have been estimated by comparing the simulated streamflow of the near, intermediate, and distant future periods under both emission scenarios with the simulated streamflow of the baseline period. The simulated average seasonal streamflow data from three GCMs (CanESM5, GFDL-ESM4, and INM-CM4-8) for the period of 2041-2060, 2061-2080, and 2081-2100 under SSP2-4.5 and SSP5-8.5 have been compared with the simulated average seasonal streamflow data of the baseline period of 2004–2023. There are four seasons: winter (December, January, February), spring (March, April, May), summer (June, July, August), and fall (September, October, November). Tables 11 and 12 describe the simulated average seasonal streamflow and relative changes in the simulated average seasonal streamflow during the

future periods under both emission scenarios compared to the simulated baseline period (2004-2023).

Table 11 The simulated average winter and spring streamflow and relative changes in simulated average winter and spring streamflow during 2041-2060, 2061-2080, and 2081-2100 under SSP2-4.5 and SSP5-8.5 compared to the simulated baseline period (2004-2023).

GCM	SSP	Period	Winter Streamflow (m^3/s)	% Change	Spring Streamflow (m^3/s)	% Change
Baseline (2004-2023)			1.20		2.38	
CanESM5	2-4.5	2041-2060	1.74	45	4.21	76.81
		2061-2080	2.17	80.8	3.67	54.36
		2081-2100	2.18	81.4	3.69	55.28
	5-8.5	2041-2060	2.54	112	3.83	60.93
		2061-2080	2.37	97.7	3.70	55.64
		2081-2100	3.13	161	4.66	95.87
GFDL-ESM4	2-4.5	2041-2060	1.91	59.3	3.23	35.66
		2061-2080	1.50	25.1	3.51	47.59
		2081-2100	1.33	10.8	3.58	50.47
	5-8.5	2041-2060	2.18	81.4	3.48	46.07
		2061-2080	2.26	88.4	4.00	67.91
		2081-2100	2.30	91.9	3.37	41.61
INM-CM4-8	2-4.5	2041-2060	1.41	17.5	3.76	58.03
		2061-2080	1.29	7.5	3.79	59.24
		2081-2100	1.43	19.1	4.11	72.55
	5-8.5	2041-2060	1.54	28.2	3.84	61.54
		2061-2080	1.40	16.3	3.76	57.94
		2081-2100	2	66.6	3.89	63.37

The results show seasonal variability in the streamflow of the Neebing River watershed. According to all three GCMs, the winter and spring streamflow is projected to increase during all the future periods under both emission scenarios compared to the simulated baseline period. The highest increase in winter streamflow is 1.34 m^3/s which is projected by CanESM5 during the 2041-2060 period under SSP5-8.5, while the lowest increase is 0.09 m^3/s, which is projected by INM-CM4-8 during the 2061-2080 period under SSP2-4.5. The highest increase in spring streamflow is 2.28 m^3/s which is projected by CanESM5 during the 2081-2100 period under SSP5-8.5, while the lowest increase is 0.85 m^3/s, which is projected by GFDL-ESM4 during the 2041-2060 period under SSP2-4.5.

Table 12 The simulated average summer and fall streamflow and relative change in average summer and fall streamflow during 2041-2060, 2061-2080, and 2081-2100 under SSP2-4.5 and SSP5-8.5 compared to the simulated baseline period (2004-2023).

GCM	SSP	Period	Summer Streamflow (m^3/s)	% Change	Fall Streamflow (m^3/s)	% Change
Baseline (2004-2023)			3.01		2.02	
CanESM5	2-4.5	2041-2060	3.12	3.65	2.33	15.15
		2061-2080	3.14	4.27	1.72	-15.20
		2081-2100	2.66	-11.54	2.13	5.34
	5-8.5	2041-2060	2.39	-20.57	1.77	-12.40
		2061-2080	2.84	-5.54	1.75	-13.40
		2081-2100	2.23	-25.76	1.89	-6.67
GFDL-ESM4	2-4.5	2041-2060	3.27	8.73	2.63	30.10
		2061-2080	3	-0.18	2.40	18.79
		2081-2100	3.07	1.92	2.37	17.16
	5-8.5	2041-2060	3.73	23.95	2.48	22.80
		2061-2080	3.56	18.22	2.96	46.19
		2081-2100	2.89	-3.99	2.69	32.91
INM-CM4-8	2-4.5	2041-2060	2.91	-3.45	2.70	33.61
		2061-2080	3.59	19.19	2.74	35.45
		2081-2100	2.88	-4.18	3.01	48.85
	5-8.5	2041-2060	3.02	0.27	2.19	8.26
		2061-2080	2.73	-9.21	2.05	1.55
		2081-2100	2.56	-15.09	2.09	3.22

The summer and fall streamflow shows variability. The summer streamflow is projected to decrease in most of the future periods, while the fall streamflow is projected to increase in most of the future periods. The highest decrease in summer streamflow is 0.78 m^3/s, which is projected by CanESM5 during the 2081-2100 period under SSP5-8.5, while the highest increase is 0.72 m^3/s, which is projected by GFDL-ESM4 during the 2041-2060 period under SSP5-8.5. The highest increase in fall streamflow is 0.99 m^3/s which is projected by INM-CM4-8 during the 2081-2100 period under SSP2-4.5, while the lowest increase is 0.03 m^3/s, which is projected by INM-CM4-8 during the 2061-2080 period under SSP5-8.5. Figure 7 illustrates the absolute changes in simulated average seasonal streamflow during the future periods under both emission scenarios compared to the simulated baseline period.

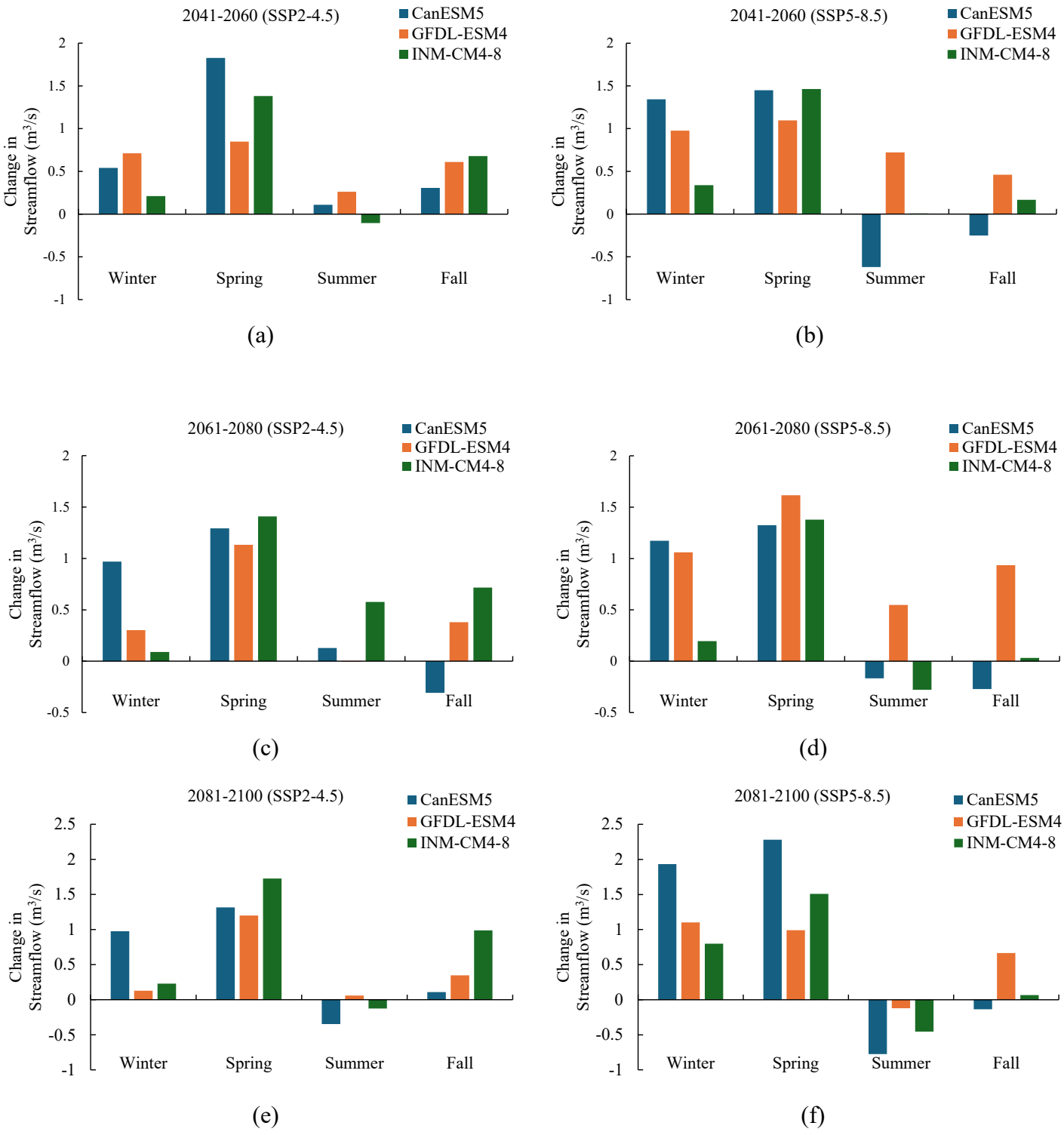

Fig. 7 The absolute changes in simulated average winter, spring, summer, and fall streamflow during (a,b) 2041-2060, (c,d) 2061-2080, and (e,f) 2081-2100 under SSP2-4.5 and SSP5-8.5 compared to the simulated baseline period (2004-2023).

4.6 Frequency of High Streamflow Events

The frequency of high streamflow events has been estimated by comparing the simulated average daily streamflow data of the baseline period (2004-2023) with the simulated average daily streamflow data of the near, intermediate, and distant future periods. The 90th and 95th percentile of the simulated average daily streamflow during the baseline period are 3.89 m^3/s, and 5.08 m^3/s, respectively. Frequency analysis of the future high streamflow events shows that, while the simulated average daily streamflow of the baseline period exceeds 3.89 m^3/s 10% of the time, and 5.08 m^3/s 5% of the time, the simulated average daily streamflow during the near, intermediate, and distant future periods under both emission scenarios exceeds this value more frequently. Table 13 describes the frequency of high streamflow events in the future periods under both emission scenarios.

Table 13 Frequency of high streamflow events during 2041-2060, 2061-2080, and 2081-2100 under SSP2-4.5 and SSP5-8.5.

GCM	SSP	Period	Frequency exceeding 3.89 m^3/s	Frequency exceeding 5.08 m^3/s
Baseline (2004-2023)			10%	5%
CanESM5	2-4.5	2041-2060	18.74%	8.38%
		2061-2080	16.61%	6.63%
		2081-2100	15.87%	6.36%
	5-8.5	2041-2060	16.15%	7.43%
		2061-2080	14.74%	7.25%
		2081-2100	23.05%	10.21%
GFDL-ESM4	2-4.5	2041-2060	13.98%	5.80%
		2061-2080	12.62%	6.40%
		2081-2100	24.06%	10.00%
	5-8.5	2041-2060	13.79%	5.87%
		2061-2080	18.66%	8.62%
		2081-2100	18.98%	6.77%
INM-CM4-8	2-4.5	2041-2060	20.30%	8.99%
		2061-2080	21.75%	10.32%
		2081-2100	13.65%	6.11%
	5-8.5	2041-2060	20.12%	10.14%
		2061-2080	18.50%	9.84%
		2081-2100	15.66%	6.73%

4.7 Frequency of Future Flooding Events

The highest observed average daily streamflow during 1953-2022 was recorded at the "Neebing River Near Thunder Bay" station on May 28, 2012, during a significant flooding event caused by a major rainstorm (Curi, 2018b). Table 14 describes the average daily streamflow recorded at the "Neebing River Near Thunder Bay" station during the 1968, 1971, 1977, 1997, 2008, 2012, and 2016 flooding events on the Neebing River watershed due to major rainstorms. During those flooding events, the observed average daily streamflow ranges between 35 m^3/s and 91.5 m^3/s.

Table 14 Streamflow recorded at the "Neebing River Near Thunder Bay" station during the 1968, 1971, 1977, 1997, 2008, 2012, and 2016 flooding events.

Date	Observed Daily Streamflow (m^3/s)
July 16, 1968	49.3
May 25, 1971	64.6
September 9, 1977	59.5
July 3, 1997	35.6
June 7, 2008	46.3
May 28, 2012	91.5
June 26, 2016	35

Considering 35 m^3/s as the threshold, the frequency of future flooding events has been estimated by comparing the simulated average daily streamflow of the baseline period (2004-2023) with the simulated average daily streamflow of the future periods. Frequency analysis shows that the average daily streamflow exceeds 35 m^3/s 12 times during the simulated baseline period, while during the near, intermediate, and distant future periods under both emission scenarios, the average daily streamflow frequently exceeds this value except in INM-CM4-8 during 2061-2080 under SSP5-8.5. The highest frequency (23 times) is predicted by CanESM5 during 2081-2100 under both emission scenarios. Therefore, it is anticipated that the Neebing River Watershed will experience more frequent flooding events in the coming decades. Table 15 describes the frequency of future flooding events in future periods under both emission scenarios, considering 35 m^3/s as the threshold.

Table 15 Frequency of future flooding events during 2041-2060, 2061-2080, and 2081-2100 under SSP2-4.5 and SSP5-8.5, considering 35 m^3/s as the threshold.

GCM	SSP	Period	no. of Occurrence >35 m^3/s
Baseline (2004-2023)			12
CanESM5	2-4.5	2041-2060	20
		2061-2080	17
		2081-2100	23
	5-8.5	2041-2060	19
		2061-2080	15
		2081-2100	23
GFDL-ESM4	2-4.5	2041-2060	19
		2061-2080	20
		2081-2100	17
	5-8.5	2041-2060	14
		2061-2080	17
		2081-2100	17
INM-CM4-8	2-4.5	2041-2060	12
		2061-2080	15
		2081-2100	18
	5-8.5	2041-2060	15
		2061-2080	9
		2081-2100	15

4.8 Magnitude of Future Streamflow Events

Considering 91.5 m^3/s as the threshold, the magnitude of future streamflow events has been estimated by comparing the observed average daily streamflow of 1953-2022 from the "Neebing River Near Thunder Bay" station with the simulated average daily streamflow of the future periods. During 1953-2022, the observed average daily streamflow never exceeded 91.5 m^3/s. Frequency analysis shows that the simulated average daily streamflow exceeds 91.5 m^3/s a number of times during the future periods. Therefore, it is anticipated that the future decades will experience high-magnitude streamflow events that have never been experienced before. Table 16 describes the frequency of high-magnitude streamflow events during 2041-2060, 2061-2080, and 2081-2100 under SSP2-4.5 and SSP5-8.5, considering 91.5 m^3/s as the threshold.

Table 16 Frequency of high-magnitude streamflow events during 2041-2060, 2061-2080, and 2081-2100 under SSP2-4.5 and SSP5-8.5, considering 91.5 m^3/s as the threshold.

GCM	SSP	Period	no. of Occurrence >91.5 m^3/s
Observed Streamflow (1953-2022)			0
CanESM5	2-4.5	2041-2060	1
		2061-2080	5
		2081-2100	1
	5-8.5	2041-2060	2
		2061-2080	0
		2081-2100	3
GFDL-ESM4	2-4.5	2041-2060	1
		2061-2080	1
		2081-2100	1
	5-8.5	2041-2060	2
		2061-2080	0
		2081-2100	1
INM-CM4-8	2-4.5	2041-2060	1
		2061-2080	2
		2081-2100	2
	5-8.5	2041-2060	2
		2061-2080	2
		2081-2100	0

Overall, the analysis of the results shows an increase in future streamflow, temperatures, and precipitation compared to the baseline period. The increase in streamflow indicates that future conditions can lead to hydrological extremes like floods. The watershed might experience more frequent and high-magnitude flooding events in the future. Moreover, the increase in temperatures and precipitation indicates that conditions can lead to frequent major storms in the coming decades. The excessive amount of stormwater might cause significant flooding as well.

5 Recommendations for Mitigation and Adaptation

Under the abovementioned circumstances, effective mitigation and adaptation strategies are essential to reduce potential flood damage in the coming decades. The following are the recommended mitigation and adaptation strategies against anticipated future flooding events.

5.1 Website

It is recommended to develop a website for the City of Thunder Bay where future flood-risk maps and inundation maps will be available and accessible to all the residents. Developing future flood-risk maps for the whole city, rather than only the floodplains, might be one of the city's most efficient flood mitigation strategies. It is recommended to develop future flood-risk maps for every ten years (2030, 2040, 2050, 2060, 2070, 2080, 2090, 2100). Flood-risk maps will help identify potential areas of the city and the timeline that might be affected by future flooding. By going through the flood-risk maps of different ten-year periods, people will understand whether their houses are in flood-risk or safe zones. Residents can take effective measures themselves to reduce flood damage rather than depending on the government. Besides, many people in Thunder Bay do not have any direct flood experience yet and might think that their houses are safe from future flooding as well. These future flood-risk maps will create awareness among the citizens of Thunder Bay. Upon reviewing these maps, residents may come to understand that while their homes may currently be safe from flood risks, this safety could be compromised in the decades ahead.

The City of Thunder Bay should also consider developing future inundation maps for every ten years (2030, 2040, 2050, 2060, 2070, 2080, 2090, 2100). These maps will help to identify the potential inundation levels of future flooding. Since different flood control strategies are effective for different inundation levels, these maps will guide homeowners to understand what mitigation strategy they must consider for their houses. Moreover, the impacts of future flooding will not be the same all over the city. Some parts might be more affected, while other parts might be less affected. Therefore, it is recommended to classify different parts of the city as different risk zones, such as high-risk zones, moderate-risk zones, and low-risk zones and different emergency plans must be prepared for those zones. The website should include these emergency plans as well.

5.2 Mobile App

It is recommended to develop a mobile application as well regarding the future flood risk of this city. By installing that app, the residents will get notifications on their cell phones prior to potential flood events in a particular area of the city. If the residents are notified about the occurrence and severity of the upcoming flood events, they might adopt effective measures in response, such as removing carpets from basements, moving furniture to the upper floors, installing flood panels on doors and basement and semi-basement windows so that floodwater does not enter the house, etc.

This mobile application might prove beneficial against flooding induced by one-day or two-day rain events that can occur anytime and anywhere in the city.

5.3 Role of Architects and Insurers

Architects can also play an important role in this city's future flood adaptation process. Basements are particularly susceptible to flood damage. The removal of basements from architectural design would not be a feasible solution as basements are used for different purposes. Besides, most of the existing buildings already have basements, and it is not feasible to get rid of them. Architects can reduce flood damage by basement renovation. It includes strengthening walls, using waterproof materials, elevating the mechanical systems above probable floodwater levels, etc. These strategies must be included in the Building Code, and their implementation must be ensured. Insurers can also play a crucial role in the adaptation process. Insurers may raise insurance rates if homeowners do not adopt preventive measures against flooding.

5.4 Compulsory Environmental Education in High Schools

Environmental Education is recommended to be made compulsory in high schools of this city so that the future generation develop environmental awareness at an early age. The future environmental challenges will mostly impact the next generations. Environmental education will influence their perceptions of environmental risk. They will become more sensitive towards environmental issues. Furthermore, environmental education will facilitate them to enhance their outlook on the environment and translate these perspectives into actions (Durmuş-Özdemir and Sener, 2016).

5.5 Permeable Gravel Driveways and Bioswales

Permeable gravel driveways are recommended to be mandatory for all residential buildings, and bioswales are recommended for all the public buildings in the City of Thunder Bay. A permeable gravel driveway has a gravel layer over a base layer, enabling water to penetrate the surface (Qin, 2020). Bioswales refer to shallow channels designed for drainage. Bioswales contain vegetation, organic matter, and riprap materials for effective water management. Rain is captured by vegetation, decreasing the total amount of precipitation reaching the ground (Xiao et al., 2017). It

is expected that during the anticipated heavy rainfall events in the future, permeable gravel driveways and bioswales will minimize runoff and store excess stormwater.

5.6 Afforestation

Afforestation is the process of creating a forest in a location that did not previously have any forest cover. This cost-effective approach focuses on reducing the consequences of climate change (Doelman et al., 2020). Forests will reduce stormwater runoff and increase flood storage capacity (Oldfield et al., 2013). There are many open spaces in the city of Thunder Bay that can be turned into forests. Considering the future climate change impacts, afforestation will be a beneficial approach for this city.

5.7 Media Influence

Media can also play an important role in the future flood adaptation process of this city. Before any potential flood event, the residents of this city might be informed through YouTube advertisements, television and radio news, and newspapers. Considering the increasing flood risks in the upcoming decades, the media can change the public perception of future flood situations through various advertisements and encourage them to adopt necessary measures.

6 Conclusion

Climate change is an undeniable fact worldwide and can potentially impact river hydrology. This study analyzes future temperature rise impacts on the Neebing River's hydrology. The SWAT model has simulated the future streamflow for 2041-2060, 2061-2080, and 2081-2100 under SSP2-4.5 and SSP5-8.5. Future climatic data have been derived from three GCMs (CanESM5, GFDL-ESM4, INM-CM4-8). The SWAT model has been calibrated and validated using SWAT-CUP. The results indicated that the model performed well. The climate projections of the watershed indicate that both temperature and precipitation will increase in the future compared to the baseline period (2004-2023). A notable effect of climate change on the streamflow has been observed. The average annual streamflow of the Neebing River Watershed has exhibited an increase in comparison to the baseline period. GFDL-ESM4 projected the highest increase in average annual streamflow, which is 49.79%, during the 2041-2060 period under SSP5-8.5. Future periods will see a decline in summer streamflow and an increase in winter, spring, and fall streamflow. The

average daily streamflow shows higher frequencies of high streamflow events. The future periods will also experience high-magnitude streamflow events. These findings suggest that the alterations in temperature and precipitation patterns will lead to a rise in streamflow within the Neebing River Watershed in the coming decades. The excess of water might result in flooding. Therefore, it is necessary to consider an organized and methodical approach to prevention and long-term adaptation against anticipated future flooding. This study recommends several non-structural, structural, and hybrid flood control strategies for the City of Thunder Bay. Community involvement will improve the efficacy of flood mitigation and adaptation strategies. If people can determine when floods might happen, they could potentially take effective measures and reduce the damage. The results of this study can assist in understanding the possible future environmental hazards associated with climate change in the Neebing River Watershed. Considering the impacts of future climate change, policymakers can adopt necessary measures. Moreover, the findings of this study can assist in developing sustainable management strategies. The outcomes of this study can also be considered in future research on the Neebing River Watershed.

6.1 Future Research Directions

One of the potential future directions of this research includes further investigation of flood magnitudes and their likelihood of occurrence using standard probability distributions that establish the connection between flood magnitudes and their probability of occurring within a defined period. Future research could look at the flashiness index as an indicator of increased variability. Moreover, future research could explore the feasibility and effectiveness of the recommended mitigation and adaptation strategies in reducing flood damage. Future research could also consider the potential land use changes in the Neebing River Watershed while simulating future scenarios.

Acknowledgments

I express my sincere gratitude to my supervisor, Dr. Adam Cornwell, for without his expertise, guidance, motivation, and continued support, this thesis would not have been possible. I would like to acknowledge sincere thanks to my co-supervisors, Dr. Kamil Zaniewski and Dr. Robert Stewart for their constant guidance. I am thankful to Dr. Pradeep Goel, Dr. Pranesh Kumar Paul,

Reg Nelson, and Tim Vehling for their suggestions. I wish to thank ClimateData.ca for providing the climate information used in this paper. ClimateData.ca was created through a collaboration between the Pacific Climate Impacts Consortium (PCIC), Ouranos Inc., the Prairie Climate Centre (PCC), Environment and Climate Change Canada (ECCC) Centre de Recherche Informatique de Montréal (CRIM) and Habitat7. This research was supported by a grant from the Ministry of the Environment, Conservation and Parks, COA Project # 9504, TPON Case No.:2020-01-1-1427550384.

References

Asadzadeh, M., Leon, L., McCrimmon, C., Yang, W., Liu, Y., Wong, I., ... & Bowen, G. (2015). Watershed derived nutrients for Lake Ontario inflows: Model calibration considering typical land operations in Southern Ontario. *Journal of Great Lakes Research*, *41*(4), 1037-1051.

Azarkhish, A., Rudra, R., Daggupati, P., Dhiman, J., Dickinson, T., & Goel, P. (2021). Investigation of long-term climate and streamflow patterns in Ontario. *American Journal of Climate Change*, *10*(4), 467-489.

Carlos Mendoza, J. A., Chavez Alcazar, T. A., & Zuñiga Medina, S. A. (2021). Calibration and uncertainty analysis for modelling runoff in the Tambo River Basin, Peru, using sequential uncertainty fitting ver-2 (SUFI-2) algorithm. *Air, Soil and Water Research*, *14*, 1178622120988707.

ClimateData.ca [Accessed on April 20, 2024]

Curi, F. (2018a). Neebing River Floodplain Mapping Update Study Hydraulics Report. *KGS Group, Final-Rev 0.*

Curi, F. (2018b). Neebing River Floodplain Mapping Update Study General Report. *KGS Group, Final-Rev 0.*

Curi, F. (2018c). Neebing River Floodplain Mapping Update Study Hydrologic Report. *KGS Group, Final.*

Daggupati, P., Shukla, R., Mekonnen, B., Rudra, R., Biswas, A., Goel, P. K., ... & Yang, W. (2018). Hydrological responses to various land use, soil and weather inputs in Northern Lake Erie Basin in Canada. *Water*, *10*(2), 222.

da Silva, M. G., de Aguiar Netto, A. D. O., de Jesus Neves, R. J., do Vasco, A. N., Almeida, C., & Faccioli, G. G. (2015). Sensitivity analysis and calibration of hydrological modeling of the watershed Northeast Brazil. *Journal of Environmental Protection*, *6*(8), 837-850.

Doelman, J. C., Stehfest, E., van Vuuren, D. P., Tabeau, A., Hof, A. F., Braakhekke, M. C., ... & Lucas, P. L. (2020). Afforestation for climate change mitigation: Potentials, risks and trade-offs. Global Change Biology, 26(3), 1576-1591.

Durmuş-Özdemir, E., & Şener, S. (2016). The impact of higher education on environmental risk perceptions. China-USA Business Review, 15(9), 459-471.

Environment and Climate Change Canada (2024a). Weather, Climate, and Hazard Historical Data. Retrieved April 28, 2024, from climate.weather.gc.ca.

Environment and Climate Change Canada (2024b). Water Level and Flow Historical Data. Retrieved April 28, 2024, from wateroffice.ec.gc.ca.

Fatehifar, A., Goodarzi, M. R., Montazeri Hedesh, S. S., & Siahvashi Dastjerdi, P. (2021). Assessing watershed hydrological response to climate change based on signature indices. *Journal of Water and Climate Change*, *12*(6), 2579-2593.

Food and Agriculture Organization of the United Nations (2023). FAO/UNESCO Soil Map of the World. License: CC BY-NC-SA 3.0 IGO. Retrieved July 15, 2023, from www.fao.org/soils-portal/data-hub/soil-maps-and-databases.

Fleury-Bahi, G. (2008). Environmental risk: Perception and target with local versus global evaluations. *Psychological Reports*, *102*, 185-193.

Füssel, H. M. (2007). Adaptation planning for climate change: concepts, assessment approaches, and key lessons. *Sustainability science*, *2*, 265-275.

Galata, A. W., Tullu, K. T., & Guder, A. C. (2021). Evaluating watershed hydrological responses to climate changes at Hangar Watershed, Ethiopia. *Journal of Water and Climate Change*, *12*(6), 2271-2287.

Gaspard, A., Simard, M., & Boudreau, S. (2023). Patterns and drivers of change in the normalized difference vegetation index in Nunavik (Québec, Canada) over the period 1984–2020. *Atmosphere*, *14*(7), 1115.

Godber, A. (2006). Local government views on addressing flood risk management on the Gold Coast. *Australian Journal of Emergency Management, The*, *21*(3), 34-40.

Hamlin, S. L., & Nielsen-Pincus, M. (2021). From gray copycats to green wolves: policy and infrastructure for flood risk management. *Journal of Environmental Planning and Management*, *64*(9), 1599-1621.

Jiménez-Navarro, I. C., Jimeno-Sáez, P., López-Ballesteros, A., Pérez-Sánchez, J., & Senent-Aparicio, J. (2021). Impact of climate change on the hydrology of the forested watershed that drains to Lake Erken in Sweden: an analysis using SWAT+ and CMIP6 scenarios. *Forests*, *12*(12), 1803.

Jones, N., & Schmidt, B. (2019). Thermal habitat: understanding stream temperature and thermal classifications.

Keller, C., Bostrom, A., Kuttschreuter, M., Savadori, L., Spence, A., & White, M. (2012). Bringing appraisal theory to environmental risk perception: A review of conceptual approaches of the past 40 years and suggestions for future research. *Journal of Risk Research*, *15*(3), 237-256.

Kiedrzyńska, E., Kiedrzyński, M., & Zalewski, M. (2015). Sustainable floodplain management for flood prevention and water quality improvement. *Natural Hazards*, *76*, 955-977.

Lakehead Region Conservation Authority (2018). Neebing River Watershed.

Lee, J. Y., Marotzke, J., Bala, G., Cao, L., Corti, S., Dunne, J. P., Engelbrecht, F., Fischer, E., Fyfe, J. C., Jones, C., Maycock, A., Mutemi, J., Ndiaye, O., Panickal, S., & Zhou, T. (2021). Future global climate: scenario-based projections and near-term information. In *Climate change 2021: The physical science basis. Contribution of working group I to the sixth assessment report of the intergovernmental panel on climate change* (pp. 553-672). Cambridge University Press.

Li, B., Tan, L., Zhang, X., Qi, J., Marek, G. W., Li, Y., ... & Chen, Y. (2023). Modeling streamflow response under changing environment using a modified SWAT model with enhanced representation of CO2 effects. Journal of Hydrology: Regional Studies, 50, 101547.

Liu, Y., Yang, W., Leon, L., Wong, I., McCrimmon, C., Dove, A., & Fong, P. (2016). Hydrologic modeling and evaluation of Best Management Practice scenarios for the Grand River watershed in Southern Ontario. *Journal of Great Lakes Research*, *42*(6), 1289-1301.

Marahatta, S., Aryal, D., Devkota, L. P., Bhattarai, U., & Shrestha, D. (2021). Application of SWAT in hydrological simulation of complex mountainous river basin (Part II: climate change impact assessment). *Water*, *13*(11), 1548.

McNeil, D., & Carson, R. (2006). The Red River Floodway Expansion Project. Proceedings of the Canadian Dam Association's 2006 Annual Conference, Québec City PQ, Sep 30 – Oct 5.

Minea, G., & Zaharia, L. (2011). Structural and Non-Structural Measures for Flood Risk Mitigation in the Bâsca River Catchment (Romania. In *Forum geografic* (Vol. 10, No. 1).

Nordbeck, R., Steurer, R., & Löschner, L. (2019). The future orientation of Austria's flood policies: from flood control to anticipatory flood risk management. *Journal of Environmental Planning and Management*, *62*(11), 1864-1885.

Oldfield, E. E., Warren, R. J., Felson, A. J., & Bradford, M. A. (2013). Challenges and future directions in urban afforestation. Journal of Applied Ecology, 50(5), 1169-1177.

Ontario Ministry of Natural Resources and Forestry (2023). Ontario Watershed Information Tool. Retrieved July 18, 2023, from www.lioapplications.lrc.gov.on.ca/OWIT/index.html?viewer=OWIT.OWIT&locale=en-CA.

Opperman, J. J., Warner, A., Girvetz, E., Harrison, D., & Fry, T. (2011, April). Integrated floodplain-reservoir management as an ecosystem-based adaptation strategy to climate change. In *Proceedings of the American Water Resources Association 2011 Spring Specialty Conference. Accessed http://www. awra. org/meetings/Baltimore2011/doc/abs/Sess* (Vol. 2030).

Pérez-Sánchez, J., Senent-Aparicio, J., Martínez Santa-María, C., & López-Ballesteros, A. (2020). Assessment of ecological and hydro-geomorphological alterations under climate change using SWAT and IAHRIS in the Eo River in Northern Spain. *Water*, *12*(6), 1745.

Poussin, J. K., Bubeck, P., Aerts, J. C. J. H., & Ward, P. J. (2012). Potential of semi-structural and non-structural adaptation strategies to reduce future flood risk: case study for the Meuse. *Natural Hazards and Earth System Sciences*, *12*(11), 3455-3471.

Provenzale, A. (2014). Climate models. *Rendiconti Lincei*, *25*, 49-58.

Qin, Y. (2020). Urban flooding mitigation techniques: A systematic review and future studies. *Water*, *12*(12), 3579.

Rahman, M., Bolisetti, T., & Balachandar, R. (2012). Hydrologic modelling to assess the climate change impacts in a Southern Ontario watershed. *Canadian Journal of Civil Engineering*, *39*(1), 91-103.

Rasid, H. (1988). Urban floodplain management in Thunder Bay: Protecting or preventing floodplain occupancy?. *Canadian Water Resources Journal*, *13*(1), 26-42.

Rasid, H., & Haider, W. (2002). Floodplain residents' preferences for non-structural flood alleviation measures in the Red River basin, Manitoba, Canada. *Water international*, *27*(1), 132-151.

Riahi, K., Van Vuuren, D. P., Kriegler, E., Edmonds, J., O'neill, B. C., Fujimori, S., ... & Tavoni, M. (2017). The Shared Socioeconomic Pathways and their energy, land use, and greenhouse gas emissions implications: An overview. *Global environmental change*, *42*, 153-168.

Saari, U. A., Damberg, S., Frömbling, L., & Ringle, C. M. (2021). Sustainable consumption behavior of Europeans: The influence of environmental knowledge and risk perception on environmental concern and behavioral intention. *Ecological Economics*, *189*, 107155.

Saddique, N., Usman, M., & Bernhofer, C. (2019). Simulating the impact of climate change on the hydrological regimes of a sparsely gauged mountainous basin, Northern Pakistan. *Water*, *11*(10), 2141.

Shrestha, S., Bhatta, B., Shrestha, M., & Shrestha, P. K. (2018). Integrated assessment of the climate and landuse change impact on hydrology and water quality in the Songkhram River Basin, Thailand. *Science of the Total Environment*, 643, 1610-1622.

Tehrani, M. J., Bozorg-Haddad, O., Pingale, S. M., Achite, M., & Singh, V. P. (2022). Introduction to Key Features of Climate Models. In *Climate Change in Sustainable Water Resources Management* (pp. 153-177). Singapore: Springer Nature Singapore.

Tingsanchali, T. (2012). Urban flood disaster management. *Procedia engineering*, *32*, 25-37.

Tucci, C. E., & Villanueva, A. O. (1999). Flood control measures in União da Vitoria and Porto União: structural vs. non-structural measures. *Urban Water*, *1*(2), 177-182.

Xiao, Q., McPherson, E. G., Zhang, Q., Ge, X., & Dahlgren, R. (2017). Performance of two bioswales on urban runoff management. Infrastructures, 2(4), 12.

Zelinka, M. D., Myers, T. A., McCoy, D. T., Po-Chedley, S., Caldwell, P. M., Ceppi, P., ... & Taylor, K. E. (2020). Causes of higher climate sensitivity in CMIP6 models. Geophysical Research Letters, 47(1), e2019GL085782.

Zeng, J., Jiang, M., & Yuan, M. (2020). Environmental risk perception, risk culture, and pro-environmental behavior. *International journal of environmental research and public health*, *17*(5), 1750.

Zhang, Y., Liu, H., Qi, J., Feng, P., Zhang, X., Li Liu, D., ... & Chen, Y. (2023). Assessing impacts of global climate change on water and food security in the black soil region of Northeast China using an improved SWAT-CO2 model. Science of the Total Environment, 857, 159482.